

WR + O binaries as probes of the first phase of mass transfer

Marit Nuijten¹ and Gijs Nelemans^{1,2,3}

¹ Department of Astrophysics/IMAPP, Radboud University, PO Box 9010, 6500 GL, The Netherlands

² Institute of Astronomy, KU Leuven, Celestijnenlaan 200D, 3001 Leuven, Belgium

³ SRON, Netherlands Institute for Space Research, Niels Bohrweg 4, 2333 CA Leiden, The Netherlands

December 3, 2024

ABSTRACT

Aims. Wolf-Rayet (WR) and O-star binaries can be the progenitors of X-ray binaries and double black hole binaries, yet their formation is not fully understood. For 21 observed WR+O systems we aim to infer if the mass-transfer started on the main sequence (Case A) or later (Case B). We also calculate (limits on) the mass transfer efficiency β , i.e. the fraction of transferred mass that is accreted and the parameter γ that denotes the fraction of angular momentum of the binary that is lost per unit mass in units of the average angular momentum of the binary per unit mass.

Methods. We infer the possible values for the initial masses based on the observed WR masses and models for WR from the literature. With these initial primary masses we can create a grid of possible periods and secondary masses for which we can determine the values β and γ would have taken for either Case A or Case B mass transfer. Based on this we can also determine which case of mass transfer is most likely for each system.

Results. Taking into account the progenitor distribution of WR+O binaries we find that highly non-conservative Case A mass transfer seems to be the most likely scenario for the majority of systems as this can explain 14 out of 21 systems. The angular momentum loss is likely relatively high (typically $\gamma > 1$). Our finding that most systems in our sample experienced case-A mass transfer is at odds with the expectation that most massive binaries go through Case B mass transfer. This suggests post-case-B systems are significantly underrepresented in the observed WR+O binary population, intrinsically or due to severe selection effects.

Key words. binaries: close - stars: evolution - stars: Wolf-Rayet - stars: massive

1. Introduction

Almost all massive stars ($\gtrsim 95\%$) have one or more companions (see e.g. Evans et al. 2011; Sana et al. 2013; Mahy et al. 2013; Kobulnicky et al. 2014; Moe & Di Stefano 2017; Almeida et al. 2017; Barbá et al. 2017; Villaseñor et al. 2021; Trigueros Páez et al. 2021; Banyard et al. 2022; Merle 2024). Roughly two-thirds of the massive stars in a binary are close enough to their companion that they will interact during their lifetime (Sana et al. 2012). This leads to many interesting phenomena. It is for instance possible for both massive stars in a binary to become a black hole (see for a review Mandel & Broekgaarden 2022). A binary with two black holes is an interesting object to study in relation to, for example, the large number of gravitational wave detections of double black holes (Abbott et al. 2023).

The formation path for black hole binaries and also high-mass X-ray binaries (e.g. Tauris & van den Heuvel 2003) typically involves a first mass transfer phase that can have crucial consequences for the following evolution (see Dorozsmay & Toonen 2024). In this paper we will focus on binaries that contain a Wolf-Rayet (WR) star and an O-star, that likely have experienced this phase (e.g. Paczyński 1967; Vanbeveren et al. 1998). Classically, WR stars are viewed as stars that have lost (most of) their envelope and therefore contain little to no hydrogen on their surface, having a high abundance of other elements, although some are found to be main sequence stars (see e.g. Martins 2023). In general, WR stars have a mass ranging from 10 to 25 M_{\odot} and have an O-star as their progenitor (Crowther 2006). WR+O binaries can be the progenitors of interesting phenomena such as X-ray binaries and the aforementioned black hole

black hole binaries (e.g. Tauris & van den Heuvel 2003; van den Heuvel et al. 2017). However, in order to understand the formation of WR+O binaries and their potential to evolve into X-ray binaries and double black holes, the mass transfer process must be understood. Two of the key ingredients of this process are the fraction of mass that is accreted by the accreting star and the fraction that is lost from the system (the mass-transfer efficiency) and the amount of angular momentum that this lost material removed from the system. The efficiency of the mass transfer can have a large influence on the evolution of the stars within the binary and the binary as a whole (see for example Shao & Li (2016)). We want to study whether it is possible to say something about the values of the mass transfer efficiency and angular momentum loss of these systems and the evolutionary phase of the donor at the start of mass transfer. Because of significant mass loss, WR+O stars in principle can also form because the WR progenitor loses its envelope via a stellar wind. However, the properties of the observed systems such as the spins of the O-stars and the orbital properties suggest that the majority of WR+O binaries have experienced mass transfer (Shara et al. 2017; Cherepashchuk 2018; Vanbeveren et al. 2018).

Mass transfer is classified depending on when in the evolution of the donor the mass transfer starts. The first type of mass transfer is Case A. This is when the donor star is still on the main sequence (MS) at the moment it fills its Roche lobe (e.g. Pols 1994; Wellstein et al. 2001; Nelson & Eggleton 2001; de Mink et al. 2007; van Rensbergen et al. 2010; Sen et al. 2022). When hydrogen burning in the core of the star has stopped, but helium burning has not yet started at the onset of mass transfer, we speak of Case B mass transfer (e.g. Paczyński 1967; van

Rensbergen et al. 2011; Podsiadlowski et al. 1992; Klencki et al. 2022). There are also cases when Case A is followed by a second phase that is Case B. These cases are called Case AB mass transfer (see e.g. Sen et al. 2022). When mass transfer starts after helium ignition in the core, it is called case C (e.g. Podsiadlowski et al. 1992). We will focus on the first two cases of mass transfer, and not on case C. This is because case C mass transfer is expected to more often be unstable than Case A or Case B (e.g. Ge et al. 2015) and here we study the formation of WR+O binaries via stable mass transfer.

Petrovic et al. (2005) studied three WR+O binaries and for all three concluded that they must have undergone Case A mass transfer. Shao & Li (2016) also studied different WR+O systems, using models. Based on their outcomes it was not possible to draw a clear conclusion on which type of system undergoes Case A or Case B mass transfer. Sen et al. (2022) study the first mass transfer phase in detail and compare their models to observations of systems that are currently transferring mass, but also show results for the systems after the mass transfer. However, all these studies compare the observed systems to one or more specific binary models. Here we take a different approach, where for each observed WR+O binary we derive what type of evolution could have led to the current system. In this way, we can constrain the fraction of the transferred mass that is lost from the system and the specific angular momentum it takes with it.

In this paper we used the VIIth catalogue of galactic WR stars (van der Hucht 2001), to choose suitable candidates to study (Sect. 3). This resulted in a sample of 21 WR+O binaries which allowed us to take a more statistical approach in studying their mass transfer. This paper is structured as follows. In Sect. 2 we introduce our method to constrain the possible progenitors of the observed WR+O binaries and the resulting mass-transfer efficiency, angular momentum loss and mass-transfer type and in Sect. 3 we introduce the properties of the binaries we study. In Sect. 4 we present the results, which we discuss in Sect. 5 and summarise in Sect. 6

2. Method

We aim to infer the mass-transfer type and (limits on) the mass transfer efficiency and angular momentum loss that the observed systems experiences. In order to do so, we need to estimate the initial masses and period of the progenitors to the WR+O binaries. In this section we will describe the methods used to estimate these initial properties of WR+O binaries. Then we will discuss how to use these initial properties to determine the mass transfer efficiency and angular momentum loss of the binary systems, as well as to determine whether the systems have experienced Case A or Case B mass transfer.

2.1. Initial masses

The observed masses of the WR and O star can be used to estimate the initial mass of the WR star in the binary. The way this is done differs between Case A and Case B. For Case B this can be done by looking at the relation between the core mass and the initial mass as found by Wellstein & Langer (1999). As a WR star consists of just the core of the progenitor star we can use this relation. Petrovic et al. (2005) made a linear fit of this relation which resulted in equation (1).

$$M_{1,i,B} = \frac{M_{WR} + 4.92}{0.53} \quad (1)$$

where M_{WR} is the mass of the WR star and $M_{1,i,B}$ is its progenitor mass for Case B.

For Case A we used figure 7 from Shao & Li (2016) to derive a similar relation. In this figure they display the relation between the current WR mass and the initial mass of that star for different initial mass ratios and initial periods. We fit a straight line that traces the lower boundary of the majority of possible masses (i.e. those in the shortest orbital periods). This resulted in the relation between the current WR mass and the initial primary mass for Case A mass transfer that can be found in equation (2). Since this relation roughly is a lower limit, that means that the outcome for $M_{1,i,A}$ based on a measured WR mass is an upper limit. This allows us to find the (approximate) initial primary mass for Case A.

$$M_{1,i,A} = \frac{M_{WR} + 4.86}{0.41} \quad (2)$$

where $M_{1,i,A}$ is the maximum progenitor mass for Case A.

With the initial mass of the WR star we can set some constraints on the parameter space of the secondary mass. For one, the current WR star has to have been the donor star for it to have lost its envelope. Since the more massive star is the donor star the initial mass of the current O star cannot be higher than the initial WR mass. Another way to get an upper limit is by using the total mass of the system. Since we assume that the O star has accreted mass, or at least not lost mass, we can state that the initial O star mass $M_{O,i} \leq M_{O,f}$, the final O star mass. From these two limits the lower of the two becomes the final upper limit for $M_{2,i}$. We can also set a lower limit to get a better restricted parameter space. To do this we can use the knowledge that the total mass of the system can not have grown, only decreased or stayed the same: the sum of the initial masses $M_{1,i} + M_{2,i} \geq M_1 + M_2 = M_T$, the current total mass, which can be rewritten to $M_{2,i} \geq M_T - M_{1,i}$. This gives the lower limit for the initial mass of the companion. If the difference is especially large this might become negative, in which case we will use 0 as a lower bound instead. Paired with the upper limit we are able to determine the range in which the initial secondary mass can be for each of our systems.

The change in both the donor mass and the accretor mass can be expressed in terms of the accretion efficiency β as $\Delta M_a = -\beta \Delta M_d$. This can also be expressed in terms of the total mass M_T and the mass ratio $q = M_a/M_d$ (Soberman et al. 1997) as follows:

$$\frac{M_T}{M_{T,i}} = \left(\frac{1+q}{1+q_i} \right) \left(\frac{1+\beta q_i}{1+\beta q} \right) \quad (3)$$

2.2. Initial period and mass-transfer type

We cannot really estimate the initial period, so we consider many possible periods. Using the estimated initial mass for both Case A and Case B we can then determine which periods lead to Case A and which to Case B mass transfer. For this, we use the fact that mass transfer starts when a star fills its Roche lobe R_L . More specifically, we use the fact that a star needs to have exhausted the hydrogen in its core before the onset of mass transfer for the mass transfer to be considered Case B. If we know the initial mass of the donor, we can determine its radius at the end of the main sequence, also called the terminal age main sequence (TAMS). This gives the condition $R_L \geq R_{d,TAMS}$ for Case B mass transfer. If the Roche lobe were to be smaller than the donor radius at TAMS, that would indicate Roche lobe overflow (RLOF)

has already happened before and the mass transfer would be Case A.

We can relate R_L to the period P and the mass ratio of the binary and the mass of the donor star M_d . For this we can make use of a relation found by Eggleton (1983) for $0.1 < Q < 10$, where Q again is the mass ratio, but inverted: M_d/M_a .

$$\frac{R_L}{a} \approx \frac{0.44Q^{1/3}}{(1+Q)^{1/5}} \quad (4)$$

And with Kepler's third law

$$P = 9.859 \cdot (1+Q)^{-1/5} M_d^{-1/2} R_L^{3/2} \left(\frac{G}{4\pi^2}\right)^{-1/2} \cdot 10^{-7} \text{d} \quad (5)$$

Here the dependence on the mass ratio Q has become small enough we set $Q \approx 1$ to simplify the expression, resulting in:

$$P \propto M_d^{-1/2} R_L^{3/2}. \quad (6)$$

With this equation we can determine the period boundary between Case A and Case B for each initial mass, setting it to the period where $R_L = R_{d,\text{TAMS}}$.

To get the donor mass and radius at the relevant points of the donor's evolution we ran a simulation of the star with Modules for Experiments in Stellar Astrophysics (MESA) (Paxton et al. 2018, and previous publications). We used the inlists provided by Klencki et al. (2020). These inlists were designed to simulate single stars from the beginning of the MS to the point in their evolution where carbon in the core was exhausted. Even though we are looking at binaries it can be a safe assumption that the stars behave roughly like single stars until one of them fills their Roche lobe and mass transfer starts. Since we only want to look at the star up until the point where it is possible for Case B mass transfer to take place, we only ran the simulations until the hydrogen in the core was exhausted (defined here as a hydrogen mass fraction in the core of less than 10^{-4}).

We only made slight alterations to the inlists as provided by Klencki et al. (2020), namely changing the initial mass and setting the metallicity to $Z = Z_\odot$. We first created pre-zero age main sequence (ZAMS) models for each Case A and Case B initial primary mass using one set of inlists. Their outcome could be used to simulate the stars from ZAMS until the helium in their core was exhausted. This gave us the parameters we were looking for to determine the boundaries for the period for both Case A and Case B mass transfer.

However, as we are not certain that solar metallicity is the correct metallicity for the systems we are studying we therefore repeated this process but with $Z = 0.5Z_\odot$. We did not study these outcomes in detail but we will briefly discuss some effects this change in metallicity has in section 5.

For more massive stars, the radius expands strongly at the end of the main sequence, making the boundary between Case A and Case B less clear. In order to take this into account, we include the end of the main sequence both in the calculations assuming Case A mass transfer as in the calculations assuming Case B.

2.3. Accretion efficiency and angular momentum loss

We now sample the parameter space of initial periods and using 200 data points within the limits for both the secondary initial masses and the initial periods, with an upper boundary of 10^3 days for the period. The minimum period is that in which

a ZAMS star would fill its Roche lobe. The values for both parameters were spaced out evenly, linear for the masses and logarithmic for the periods. For each of the initial period and mass estimates we can derive the accretion efficiency β and the loss of angular momentum in terms of the binary's specific angular momentum loss per unit mass of the binary

$$\gamma = \left(\frac{\Delta J_{\text{lost}}}{\Delta M_{\text{lost}}}\right) \left(\frac{M}{J}\right) \quad (7)$$

An equation for β is fairly straightforward using equation 3. After multiplying both sides by $(1+\beta q)$ and rearranging the terms we get an equation where it is only dependent on the initial and current masses of the system:

$$\beta = \left(\frac{1+q}{1+q_i} - \frac{M_T}{M_{T,i}}\right) \left(q \frac{M_T}{M_{T,i}} - q_i \frac{1+q}{1+q_i}\right)^{-1} \quad (8)$$

We can also relate the angular momentum loss γ to the periods and masses of the WR+O binary and its possible progenitors. For this we use two equations, Kepler's third law to relate P/P_i and $M_T/M_{T,i}$ to the change in semimajor axis a/a_i . This change can be related to γ under the assumption that γ is constant over time (Pols & Marinus 1994):

$$\frac{a}{a_i} = \left(\frac{M_d}{M_{d,i}} \frac{M_a}{M_{a,i}}\right)^{-2} \left(\frac{M_T}{M_{T,i}}\right)^{2\gamma+1} \quad (9)$$

This can be then be equated to the relation for a/a_i from Kepler's third law and rewritten to give an equation for gamma that relates the period and masses of a WR+O binary and its prior:

$$\left(\frac{M_d}{M_{d,i}} \frac{M_a}{M_{a,i}}\right)^{-2} \left(\frac{M_T}{M_{T,i}}\right)^{2\gamma+1} = \left(\frac{M_T}{M_{T,i}}\right)^{1/3} \left(\frac{P}{P_i}\right)^{2/3} \quad (10)$$

$$\left(\frac{M_T}{M_{T,i}}\right)^{2\gamma+\frac{2}{3}} = \left(\frac{P}{P_i}\right)^{2/3} \left(\frac{M_d}{M_{d,i}} \frac{M_a}{M_{a,i}}\right)^2 \quad (11)$$

$$(12)$$

so

$$\gamma = \log_{M_T/M_{T,i}} \left(\left(\frac{P}{P_i}\right)^{1/3} \frac{M_1 M_2}{M_{1,i} M_{2,i}} \right) - \frac{1}{3} \quad (13)$$

2.4. Limiting the possible solutions

The size of the grid is quite large so it can be useful to limit the part of the grid we are interested in so we can study that in more detail. To start with, we disregarded all points where $\gamma < 0$ since that would mean the system has gained angular momentum in some way. We also used an upper limit of $\gamma < 5$ since values higher than that limit are probably nonphysical. We can see this when we look at mass loss through a circumbinary ring as in Soberman et al. (1997):

$$\gamma = \frac{M_T^2}{M_d M_a} \cdot \frac{a_r^{1/2}}{a} \quad (14)$$

Here a_r is the radius of the ring. If we would take $\gamma = 3$ and $M_1 = 20M_\odot$ and $M_2 = 10M_\odot$ we would get a radius of the ring a_r that is 4 times as big as the radius of the binary. At some point one can start to wonder if that is still a reasonable radius for a circumbinary disk to have, is it still circumbinary or just a disk? For $\gamma = 5$ this radius becomes even bigger: $a_r \approx 11.1 \cdot a$. As we

do not think a circumbinary disk with such a radius is physically plausible we used this value for γ as an upper limit. We only consider points where $0 < \gamma < 5$ and deem high values ($\gamma > 3$) unlikely.

The critical q values further limit the parameter space. For $q > q_{\text{crit}}$ mass transfer will become unstable. When that happens we do not expect the binary to have become a WR+O binary. We can therefore also disregard the areas where $M_{1,i}/M_{2,i} > q_{\text{crit}}$. However, the exact value is hard to determine, as it is dependent on a lot of variables such as the stellar radius and the mass, but also properties such as the efficiency and the case of the mass transfer. Ge et al. (2015) have determined q_{crit} values for a range of different scenarios for conservative mass transfer. They find the critical q value for a $16M_{\odot}$ primary star can range from 1.793 to 8.646. We do not expect the systems we will be studying to have undergone conservative mass transfer, therefore we will not use this range for q_{crit} . But it does show there might not be a single correct value for this critical q but instead a range for both Case A and Case B. We disregard results that lie outside the strictest boundary, but we do take into account the part that is in between that and the most forgiving boundary.

From the literature we find the following ranges to be satisfactory for either Case A or Case B mass transfer respectively (Gallegos-Garcia et al. 2022; Klencki et al. 2021):

$$\begin{aligned} 1.6 &\leq q_{\text{crit,A}} \leq 3 \\ 4 &\leq q_{\text{crit,B}} \leq 10 \end{aligned}$$

Finally, detailed studies (e.g. Sen et al. 2022) find that very close binaries lead to a merger of the two stars independent of their mass ratio. The limiting period is not very certain and depends on assumptions, but the lower range of Case A periods is very likely ruled out too.

2.5. Most likely progenitors

We also take into account prior information known about the most common properties of binary systems similar to those of the WR+O star progenitors. The properties we take into account are the mass ratio and the period. To get this information we used the COSMIC code by Breivik et al. (2022) and the results of Moe & Di Stefano (2017) to create a sample of O+MS binaries with a size of 10^5 and $M_{1,\text{min}} = 16$. This was to ensure that the primary would be an O star and the sample was large enough. The random seed of the sample was 20. Since these type of binaries are expected to be the progenitors of the WR+O binaries we studied we can use this distribution to say something about the likelihood of different scenarios we might find for the progenitor evolution such as the initial secondary mass. We can do this by studying the distribution of the O+MS mass ratios and periods. In figure 1 a 2D histogram of the period and the mass ratio of the sample is shown. In the sample we used a range for the primary mass ($16M_{\odot} < M_1 < 150M_{\odot}$) such that the initial primary star is an O-star and $q > 1$ since we want the O-star to be the donor and therefore to be the heavier initial star.

From the distribution we can see that the closer to $q = 1$ we get the more binaries there are in particular for the systems with periods below several tens of days. For periods there is a clear preference for lower periods of $\log P \lesssim 4$, and slightly so for $\log P \lesssim 2$. Following these results we would therefore expect the progenitors of the WR+O binaries to most likely have a mass ratio close to one and an orbital period that is not too high. This does of course not mean that these are the only values the progenitors can have, but it does say something about which values

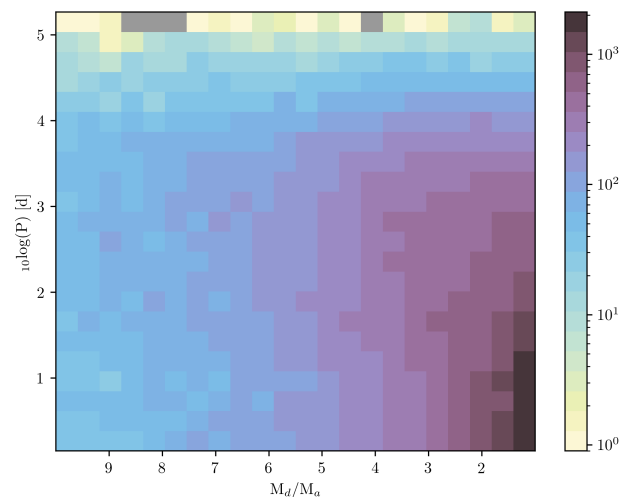


Fig. 1. The period and mass ratio distribution for a sample of 10^5 O+MS systems where $16M_{\odot} < M_1 < 150M_{\odot}$ and $q > 1$, based on the distributions found by Moe & Di Stefano (2017). The colour bar gives the number of systems per cell.

are more likely than others to have occurred. We can use this result to say something about the likelihood of certain scenarios we might find in our results. Scenarios with lower q will be more likely based on this O+MS distribution.

A final thing we can look at for this distribution is which systems we expect to undergo Case A mass transfer and which systems we do not expect this for based on our calculated period boundary between Case A and B. About one-third of the O+MS systems (36,44%) is expected to undergo Case A mass transfer, while the other two-thirds have too large initial periods for them to undergo Case A mass transfer. If all O+MS binaries have an equal likelihood to become a WR+O binary and the observed WR+O binaries we studied are not too severely biased we would expect most of them to not have undergone Case A mass transfer.

3. Objects

The systems we study are all taken from the VIIth catalog of galactic Wolf-Rayet stars by van der Hucht (2001). This is a catalog containing all the WR stars that are in the Milky Way. This iteration contains a total of 226 WR stars. We filter the WR stars in the catalog using the following criteria:

- The WR star is in a binary
- Its companion is an O-star
- The orbital period of the system is known
- Both the primary and secondary mass are known

Besides the WR star being in a binary, we want its companion to be an O-star since those systems could likely be progenitors of double black hole binaries. To be able to say something useful about the remaining WR+O systems that are in the catalogue, we need some additional information: the masses of both stars and their orbital period. However, the catalogue does not contain information on the stellar masses for all binaries. We therefore had to get those masses from other sources and those are indicated in the table.

This results in a sample of 24 WR+O binaries in the Galaxy. Initially this was the sample we were working with. However, as we were running simulations of the WR progenitor stars it turned out some of the progenitors were too heavy to do this properly.

WR#	Spectral type	Binary status	P (d)	M_{WR} (M_{\odot})	M_O (M_{\odot})	q	R_L (R_{\odot})
9	WC5+O7	SB2	14.3	9	32	0.28	23.45
11	WC8+O7.5III-V	SB2, VB	78.5	9.0 ± 0.6^a	28.5 ± 1.1^a	0.32	73.24
21	WN5o+O4-6; WN5o+O7V	SB2	8.25	19	37	0.51	21.32
30	WC6+O6-8; WC6+O7.5	SB2	18.8	16	34	0.47	34.73
31	WN4o+O8V	SB2, VB	4.83	$>11^b$	$>24^b$	0.46	12.37
35a	WN6 + O8.5 V	SB2	41.9 ^c	19 ^c	18 ^c	1.1	45.1
42	WC7+O7V	SB2	7.89	14	23	0.61	18.84
48	WC6(+O9.5/B0Iab); WC6+O6-7V	SB1, VB	19.14	18 ^d	29 ^d	0.62	37.03
62a	WN4-5o; WN5+O5.5-6; WN6o	SB2	9.1	$>21.5 \pm 4.8$ (of $>22.6 \pm 5$) ^e	$>38.7 \pm 5.2$ (of $>42.0 \pm 5.0$) ^e	0.55	24.03
68a	WN6o+O5.5-6; WN6o	SB2	5.22	$>15 \pm 5^f$	$>30 \pm 4^f$	0.50	14.50
79	WC7+O5-8	SB2, VB	8.89	11	29	0.38	18.45
97	WN5b+O7	SB2	12.6	2.3	4.1	0.56	14.04
113	WC8d+O8-9IV	SB2	29.7	13	27	0.48	44.00
127	WN3b+O9.5V	SB2	9.56	17	36	0.47	22.58
133	WN5o+O9I	SB2, VB	112.8	9.3 ± 1.6^g	22.6 ± 3.2^g	0.13	92.42
137	WC7pd+O9; WC7ed+O9	SB2	4763.25	4.4 ± 1.5^h	20 ± 2^h	0.22	882.00
139	WN5o+O6III-V	SB2	4.2	9.3	28	0.33	10.53
140	WC7pd+O4-5; WC7ed+O5	SB2, VB; CWB	2898.1	16 ± 3^i	41 ± 6^i	0.39	990.97
151	WN4o+O5V	SB2	2.13	20	28	0.71	8.94
153	WN6o/CE+O6I; WN6o/CE+O3-6+B0:I+B1:V-III	SB2 + SB2	$6.69 + 3.47$	$>6^k$	$>21^k$	0.29	7.97
155	WN6o+O9II-Ib	SB2	1.64	24	30	0.80	8.03

Table 1. All data from van der Hucht (2001) plus a: North et al. (2007), b: Vanbeveren et al. (2020), c: Gamen et al. (2014), d: Lenoir-Craig et al. (2021), e: Collado et al. (2013), f: Collado et al. (2015), g: Richardson et al. (2021), h: Lefèvre et al. (2005), i: Fahed et al. (2011), k: Demers et al. (2002)

These were the progenitors of the three systems with $M_{WR} \geq 45M_{\odot}$, WR22, WR47 and WR141. The other 21 have $M_{WR} \lesssim 25M_{\odot}$. The high WR masses of the three systems result in initial primary masses of $M_{1,i} \gtrsim 100M_{\odot}$. These initial masses proved to be too heavy to run proper simulations of the donor star from ZAMS to TAMS later on. Therefore, we discarded these three systems from our selection. WR35a was found to be a binary after the latest version of the van der Hucht (2001) by Gamen et al. (2014).

An overview of the final sample consisting of 21 WR+O binaries and some of their properties can be found in table 1. When no source is specified that means the data is taken from van der Hucht (2001). The mass ratio was determined using the masses and the Roche lobe radius of the WR star R_L is determined using Eq. 5.

4. Results

We present the results of our study in figures per object. As an example we use WR9 shown in figure 2. The main graph is divided into two parts, the upper half for Case B and the lower half for Case A. The initial mass of the WR star as estimated is given in a box for each of the two cases. The x-axis at the bottom shows initial secondary masses covering the allowed ranges (see Sect. 2.1) for both of the cases. The y-axis shows the range of

the initial periods. The colour gradient within the parts for Case A and B displays the γ values we found for each point in the grid of initial secondary masses and periods for both Case A and Case B, with a colour bar on the side showing the legend. Every integer value of γ is marked with a black line for clarity. Values of γ below 0 (white) and above 5 (black) we consider as ruled out. Some parts of the grid appear more shaded out than others. These shaded areas indicate the critical q values. The parts without shading will always experience stable mass transfer based on the q_{crit} range used. The partly shaded out parts could have experienced both stable or unstable mass transfer, depending on which exact value for q_{crit} we would take. The parts that are shaded out heavily will always experience unstable mass transfer based on the critical q values. For the part of the graph that displays the grid for Case B we show the lower limit that P_i needs to have for Case B mass transfer to occur as the dashed line. There is also the part below the dashed line where the shaded areas are different than for the rest of the graph, representing late Case A mass transfer that may behave more like Case B due to the composition of the donor. It is unclear if the critical q values then also would be those of Case B. Therefore we (also) show the critical q values of Case A. These do not correspond to the same possible values for the initial secondary mass $M_{2,i}$ of the lower, Case A, part of the graph. That is due to the fact that the initial mass of the primary M_i is different and therefore the mass ratio q is also different. Lastly, there is a smaller graph at the bottom that displays the mass transfer efficiency β for both cases

of mass transfer, depending only on the initial secondary mass and not on the initial period. This graph uses the same values for the x-axis as the other two graphs does. The y-axis displays the value for β for a certain mass ratio q .

For each observed system we can now look which of the two mass-transfer types is possible and what the possible and likely values of β and γ are. We present the results according to the possibilities.

4.1. Mass-transfer type

4.1.1. Case A more likely

There are many systems for which we conclude that Case A is the most likely, and this is the largest part of our sample. From the 20 systems we studied, 14 fall into this category based on our results: WR9, WR21, WR30, WR31, WR42, WR48, WR62a, WR68a, WR79, WR127, WR139, WR151, WR153 and WR155.

As an example we will look at WR9 (figure 2). The results for the other systems can be found in appendix A. For this system, Case B is not fully excluded, but to have experienced Case B, it would take on extremely high values ($\gamma \gtrsim 4$) which while not impossible are not plausible. A similar conclusion holds for the other systems in this category. Instead, the Case A results are possible in the sense that values of γ in the expected range are found. For the late Case A results (top panel below the dashed line) there are also solutions with plausible γ values for many of the systems, while for others the γ values are rather high again ($\gamma \gtrsim 3$).

For all systems there are some limits imposed by the critical q values concerning which progenitors would have undergone stable Case A mass transfer. The degree in which these limits affect the possibilities differ for each system, but for all systems there are options towards the upper limit of the secondary mass, depending on which value for the critical q is assumed. However, for about half of these systems stable Case A evolution is only possible if the higher critical q value of 3 is true. These systems, WR31, WR42, WR48, WR62a, WR68a, WR151 and WR155 have the most unequal initial mass ratios and all have rather short periods (but overlapping with the other systems). We should note here that the progenitor mass we use for Case A is an upper limit. Lower progenitor masses make the initial mass ratio lower and thus allow for more stable mass transfer. The expected progenitor distribution, peaking towards shorter periods and more equal masses puts the a priori most likely progenitors also in the region where stable Case A mass transfer is possible. This would be the scenarios where the mass transfer efficiency most likely would have been very low. We will discuss the mass transfer efficiency for all systems in more detail in section 4.2. We repeat here that towards the bottom of the Case A box the systems likely merge (see section 2.4).

Taking all of this into account we can say that, based on the values for γ we can exclude Case B mass transfer as a plausible scenario for these 14 systems. Case A mass transfer with a low mass transfer efficiency seems to be the most likely scenario for these binaries based on our results.

4.1.2. Case A and Case B possible

There are also systems in our sample where we were not able to say which cases of mass transfer was most likely as both Case A and Case B seem possible. Of the systems in our sample we found 3 where this is the case: WR11, WR113 and WR133. WR35a is marginally also in this class, as there is a small range

Average ang. mom. loss γ for WR9, where $M_{WR}=9$, $M_O=32$, $P=14.3$

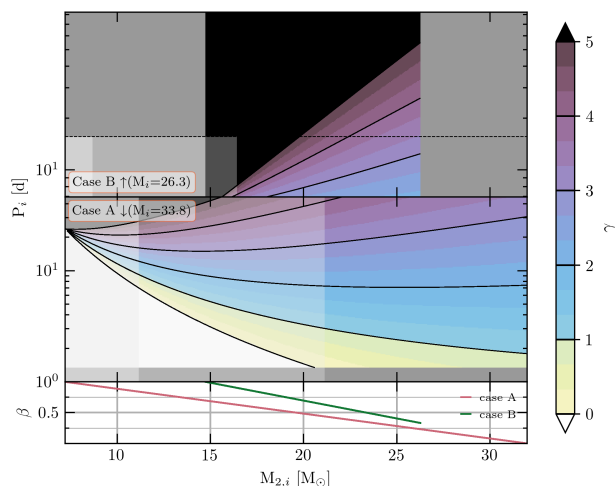


Fig. 2. The resulting values for γ (colour) and β (lines in lowest graph) for the initial parameter space of WR9. Each integer value of gamma is marked with a solid line. The shaded boxes indicate whether mass transfer will be stable. Parts without shading will be stable, lightly shaded parts can be both stable or unstable, depending on the exact value of q_{crit} . The heaviest shaded parts will always experience unstable mass transfer. The dashed line indicates the period boundary for Case B. Dark grey shades indicate excluded mass ranges (see text).

of Case A allowed. However, Case B seems more likely for that system (see below). We will examine the plot WR11 as an example (figure 3). The plots containing the other results can be found in appendix A.

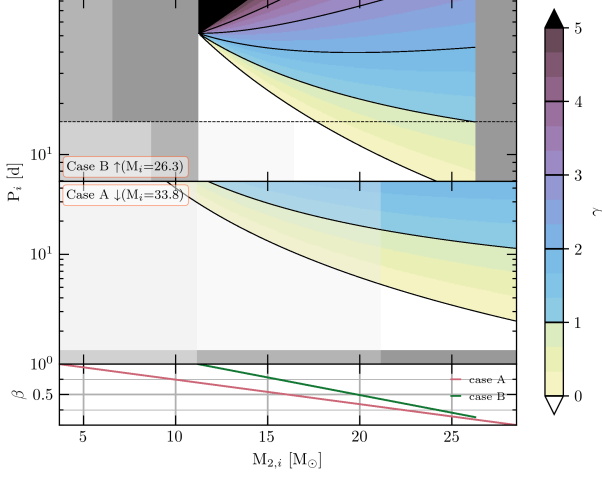
For these three systems we can see that for both Case A and Case B there are many possibilities where the mass transfer would have been stable regardless of which value for q_{crit} is assumed. While it does pose some limits for Case A it still leaves enough possibilities. The values for γ are also within reason ($\lesssim 3$) for Case A and large parts of the Case B grid. The last thing we could use to see if one case of mass transfer might be more likely than the other is to compare the results to the progenitor distribution. This distribution tells us that we are most likely to see low initial mass ratios with initial periods that are also not very high, although for the Case B region the mass ratios are more equally distributed (see Fig. 1). While this would shift the preference to a lower β for Case A, it does not impose any other limits for these three systems that would make either Case A or Case B very unlikely. That is because even for low q and P there are still plausible scenarios for both cases of mass transfer to be found.

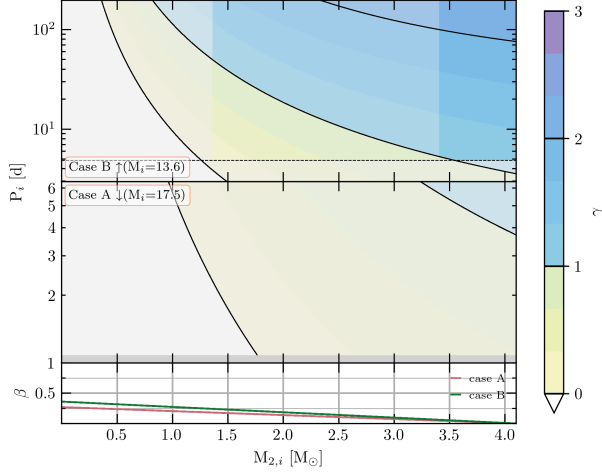
With that we are out of options within our results to rule out any of the two cases of mass transfer. Therefore these systems might have undergone either Case A or Case B mass transfer based on our results.

4.1.3. Case A not possible

Instead of Case A being more likely we also have two systems where based on our results we deem Case B mass transfer to be the most likely scenario. These systems are WR97, WR35a and WR140.

We follow the same procedure by looking at γ and q_{crit} . For WR97 (figure 4) all possible Case A progenitors are predicted to undergo unstable mass transfer even by the most lenient q_{crit} value and therefore we can exclude those as a possibility. For

Average ang. mom. loss γ for WR11, where $M_{WR}=9$, $M_O=28.5$, $P=78.5$

Fig. 3. The same as figure 2 but for WR11.

Average ang. mom. loss γ for WR97, where $M_{WR}=2.3$, $M_O=4.1$, $P=12.6$

Fig. 4. The same as figure 2 but for WR97.

Case B there are also some limitations set by the critical q values for this system, but there is still a part where it is certain mass transfer will be stable with reasonable γ values. WR97 is peculiar in the sense that the masses of both the WR and the O-star are quite low.

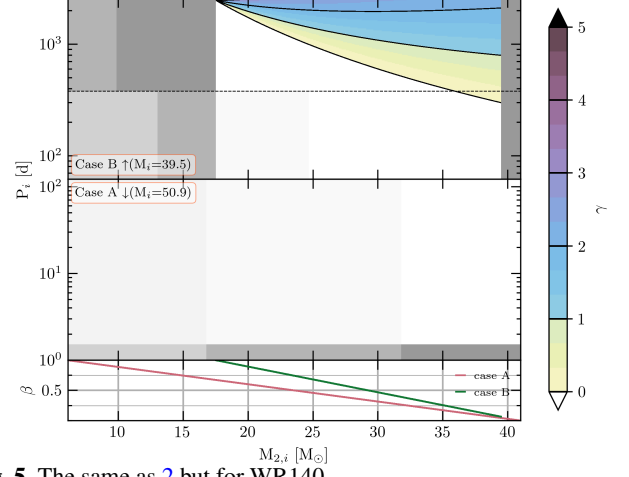
For WR35a (see appendix A) there is a small range of possibilities for Case A, but Case B is more likely. Due to the high current mass ratio, only low values of β are possible.

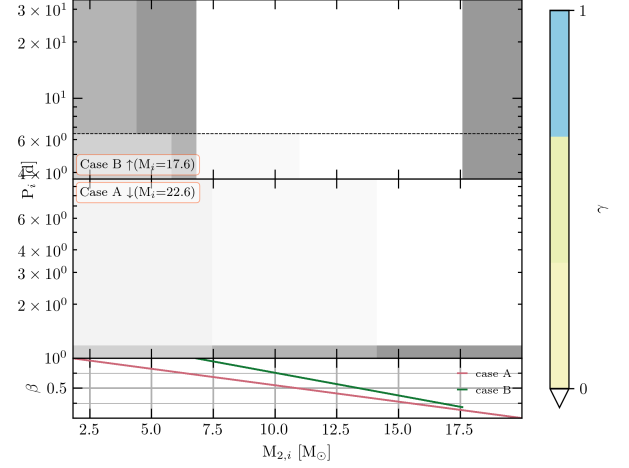
For WR140 (figure 5) there are also options for Case B, but the situation is different. For Case A there are no solutions with positive γ . This is a consequence of the very wide period of the system, which makes that it could even have been case C or even have avoided mass transfer all together.

Finally, for WR 137 (figure 6) we find that both Case A and Case B do not seem likely scenarios. There simply are no solutions, because of the very wide period of the system. As in the case of WR 140, mass transfer may have been avoided.

4.2. Mass transfer efficiency and angular momentum loss

One way in which we can determine the possible mass transfer efficiencies of a system is by using the q_{crit} values for each case

Average ang. mom. loss γ for WR140, where $M_{WR}=16$, $M_O=41$, $P=2898$

Fig. 5. The same as 2 but for WR140.

Average ang. mom. loss γ for WR137, where $M_{WR}=4.4$, $M_O=20$, $P=4763$

Fig. 6. The same as figure 2 but for WR137.

of mass transfer as an upper limit. This is done by determining the expected β for each system for both cases of mass transfer as a function of the initial secondary mass. This can then be combined with the critical q values for both Case A and Case B to allow us to get an upper boundary for each system. However, since we have a range of values for q_{crit} instead of one, that means we will also get a range for β_{max} . For the lower and upper boundary of q_{crit} we can find the matching mass transfer efficiency and use that as an upper limit. For Case A this corresponds to $1.6 < q_{crit,A} < 3$ and for Case B to $4 < q_{crit,B} < 10$. An overview of the matching upper limits for β for each binary is given in table 2. We only gave the limits for cases of mass transfer we found to be plausible. More detail on how we determined this can be found in previous sections.

For Case A we expected to find higher mass transfer efficiency with values ranging from $\sim 0.1 - 0.7$ while for Case B we expected to find lower values of $\lesssim 0.25$ for the efficiency (e.g. Sen et al. 2022; Shao & Li 2016; de Mink et al. 2007). For the Case A results, the efficiency is a combination of a low efficiency of the fast mass-transfer phase and a higher efficiency in the slow phase (see Sen et al. 2022). However, when we look at the values we find for β_{max} for the systems we studied we find something different. Firstly, the upper limits we find for Case B are often very high ($\gtrsim 0.9$) independent of which value for q_{crit} is

WR#	$q_{\text{crit,A}} = 3$	$q_{\text{crit,A}} = 1.6$	$q_{\text{crit,B}} = 10$	$q_{\text{crit,B}} = 4$
9	0.84	0.44		
11	0.70	0.30	1.00	1.00
21	0.46	0.01		
30	0.49	0.06		
31	0.41	0.00		
35a	0.02	0.00	0.58	0.33
42	0.25	0.00		
48	0.28	0.00		
62a	0.43	0.00		
68a	0.42	0.00		
79	0.59	0.18		
97			0.24	0.06
113	0.41	0.00	1.00	0.89
127	0.51	0.07		
133	0.45	0.04	1.00	0.90
137				
139	0.66	0.26		
140			1.00	1.00
151	0.20	0.00		
153	0.60	0.22		
155	0.15	0.00		

Table 2. The upper limits for β as determined by q_{crit} for Case A and Case B mass transfer. The limits are only displayed for the case(s) of mass transfer that we found to be plausible. Depending on which value for q_{crit} is chosen, the upper limit of β is different. What is certain is that β_{max} falls somewhere between the two values for each case that are displayed in this table. Other parameters like γ are not taken into account for these limits.

taken. This seems to contradict the expectations we had of finding $\beta \leq 0.25$ for Case B for one of the systems where we expect Case B to be the most likely scenario, WR140. However, that the maximum value is high does not automatically have to mean that this is also the efficiency that the mass transfer had. For WR97 and WR35a, we do find low maximum values of β .

For Case A we find very different values for β_{max} . The majority of the systems we studied has $\beta_{\text{max}} < 0.5$ even for the most lenient value of q_{crit} . The strictest boundary leaves no systems with $\beta_{\text{max}} > 0.5$ and roughly half of the systems with $\beta_{\text{max}} \sim 0$ which would implicate that Case A mass transfer having taken place is not the most likely scenario for those systems combined with those critical q values. These results are also not perfectly in line with the expectations we had, just as for Case B. We expected values of $\beta_{\text{max}} \sim 0.1 - 0.7$. While these possibilities again are not excluded by our results, a lower maximum seems the more likely scenario based on our results. This is supported even more when we again take into account the progenitor distribution and the higher likelihood of lower q and with that lower values for β .

Therefore we find that at least for Case A mass transfer the mass transfer efficiency was most likely low due to the progenitor distributions and even more so because of the limitations posed by q_{crit} .

We can also look at the most likely values for γ , as this is a parameter that is often fixed to a certain value or it is assumed that the mass that is lost takes away the angular momentum of the accretor. For binaries with initial mass ratios not far from unity, the latter implies values of γ around 1. The transition from γ from below to above unity is visible in most of the figures, implying that values around unity indeed are possible. However, the low γ values typically come from initially short periods that

may very well lead to mergers, suggesting higher γ values above 1 are more likely. When viewing the figures in the appendix, some systems (WR31, WR35a if it was Case B, WR139, WR79, WR151, WR153 and WR155) only have solutions of γ above 1. We should note here that our initial masses of the WR progenitors are upper limits (see Sect. 2.3, and lower initial masses lead to somewhat lower values of γ (Eq. 13).

5. Discussion

Here, we will discuss what assumptions were made in our work and their possible influence on the results and conclusions.

Firstly we assumed that the companion star did not or could not have lost mass with respect to its initial mass. However, that is not totally correct, stars can lose mass through stellar winds. While the amount of mass that is lost in this way is not expected to be large, it does mean that it is possible the secondary star has slightly decreased in mass with respect to its initial mass $M_{2,i}$.

Another caveat that has to do with the mass is the way in which the masses of the WR progenitors are determined for both Case A and Case B mass transfer. We used a linear relation for each as explained in 2. These relations are an approximation. While the initial progenitor masses are close to the outcomes of these equations they might also be a little lighter or heavier than the masses we used for our results. However, by including part of the Case A parameter range in the top panels of the plots we cover a significant fraction of this uncertainty. Another factor for this uncertainty is that some of the WR and O-star masses are uncertain as can be seen in section 3. We did not systematically vary the masses but the effect of the changes of the mass is as follows: lower WR masses move the curves down in the figures, i.e. increase the values of γ . Increasing the O-star masses has the same effect. We therefore do not expect a specific bias in our results, apart from the one mentioned above due to our Case A progenitor masses being upper limits.

We assumed a solar metallicity for the systems that we studied although we are not fully certain that that is accurate. We therefore also looked at what effect a lower metallicity might have on the most likely scenario for a system. The outcomes for β and γ for a certain combination of initial parameters will not be altered as those are not dependent on metallicity. However, the period boundaries are dependent on the radius of the star at certain points in its evolution which does change with metallicity. The resulting core masses also depend on the metallicity.

We ran the simulations to determine these boundaries again but for $Z = 0.5Z_{\odot}$. For these simulations, the radius of the star at TAMS will be smaller for a lower Z , this radius is indicated with the dot for each track. Because of this, the values for P_i will also become smaller.

What this difference in evolution means for our results can be seen in a new figure for WR11 to illustrate the effect (figure 7). We see that there are less possible scenarios for both Case A and B. Maybe more interestingly, for Case B lower and more plausible values for γ become possible within these new boundaries, whereas the possibilities for the initial period get drastically smaller for Case B. At the same time, the conclusion that $\gamma > 1$ is most likely changes as there now is an upper limit on γ just above 1. Based on these results we can therefore say that a different metallicity could influence the likelihood of the four scenarios we have studied and our conclusion on the most likely value of γ . It might be interesting to study this in more detail in future research.

Lastly there also is the uncertainty in the exact value for critical q above which mass transfer will become unstable. We used

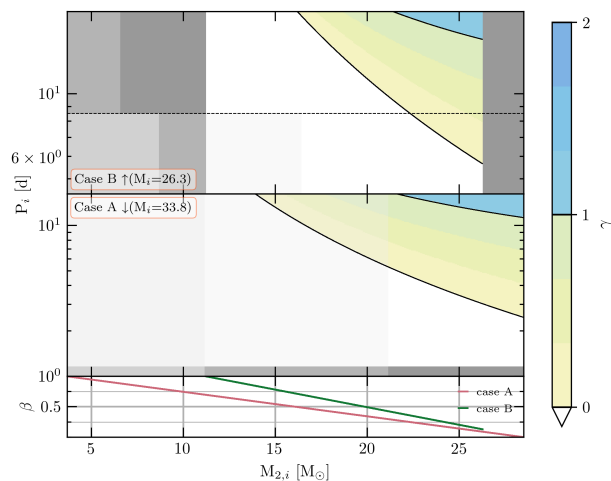
Average ang. mom. loss γ for WR11, where $M_{WR}=9$, $M_O=28.5$, $P=78.5$


Fig. 7. The same as figure 3 but for a metallicity of $Z = 0.5Z_{\odot}$.

different values found in the literature and all values in between as a possible range, but in reality there is a single value of q_{crit} for each system that is able to determine whether the mass transfer will be unstable or not. Since it requires a lot of information to accurately determine this, as can be seen in e.g. Ge et al. (2015), it was not possible for us to do so as we did not have all of the required information. Therefore these regions provide an uncertainty on which progenitors may be possible for stable mass transfer for both Case A and Case B mass transfer. We already mention this briefly in the results but it is important to keep in mind when interpreting the results.

6. Conclusion

The goal of this research was to look into what type of mass transfer WR+O binaries might have experienced in the past and what the mass transfer efficiency might have been. For this we used the knowledge that their progenitors are O+MS binaries and that these binaries are most likely to have a low mass ratio q . Using this and the other possible restrictions discussed in 2 we studied 21 WR+O binaries and their possible cases of mass transfer, the efficiency β and the angular momentum loss.

With regards to which case of mass transfer the WR+O binaries might have experienced we differentiated between three different scenarios: most likely Case A, both Case A and Case B plausible and Case A not plausible. The first scenario was the largest group in our sample with 14 out of 21 systems having most likely experienced Case A mass transfer based on our results. The other two groups have many fewer systems in them.

For the systems experiencing Case A (i.e. the majority of cases), we find the mass transfer efficiency to have been low and unlikely a fixed value (as found by de Mink et al. 2007). For Case B values up until 1 are possible for some systems while for Case A the highest possible value we found as being possible is $\beta_{max} = 0.84$.

This is not what we expected from analysing the distribution of O+MS binaries, as we only expect about one-third of those systems to undergo Case A mass transfer. It could be that our sample is not complete enough to get progenitors representative of O+MS binaries, but it may suggest the products of Case B mass transfer do not contribute in the same way to the observed WR+O star population as the post-case-A systems. Post case-B binaries tend to have longer periods which are harder to

measure spectroscopically. However, some objects in our sample have long periods so the selection effect can be subtle. One effect that could hide post Case B systems may be that the stripped stars remain cool for longer (Dutta & Klencki 2024). Based on our results we cannot draw a conclusion on which of these things is the cause of this discrepancy or whether it is caused by selection effects.

With these results we come to the conclusion that the observed WR+O binaries are most likely to experience Case A mass transfer but Case B is also a possibility for some. This is not representative of which case of mass transfer we expect their progenitors (O+MS binaries) to undergo.

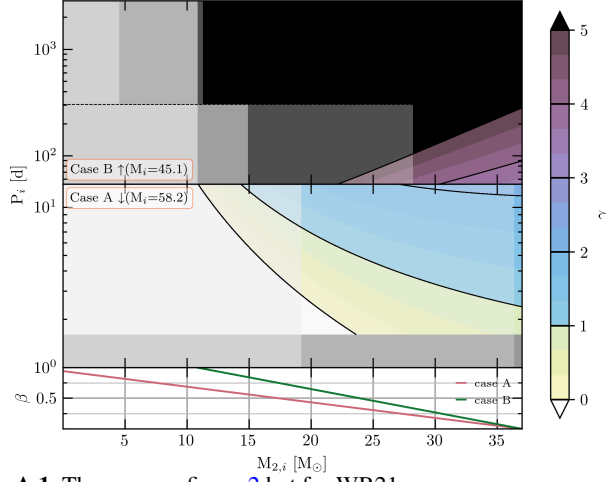
The values of γ cannot be determined accurately, but values above 1 are implied for most cases. However, lower metallicity would lower the estimates of γ .

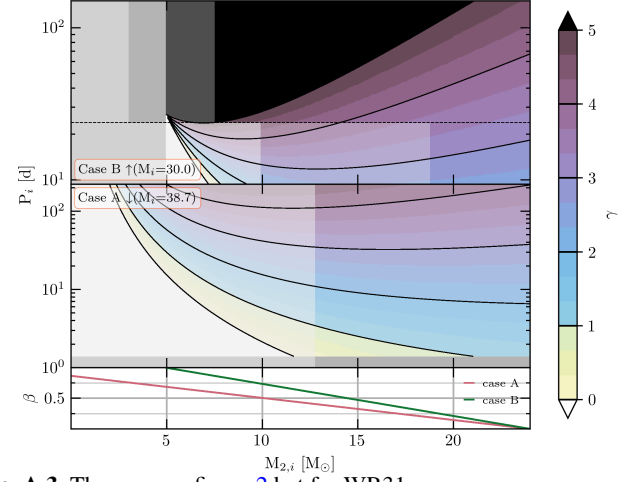
Acknowledgements. We thank the referee for detailed comments that improved the paper. We would like to thank Alina Istrate for her help and advice on using MESA and for her advice in general. We also would like to thank Jakub Klencki for helpfully answering some of our questions. G.N. is supported by the Dutch science foundation NWO.

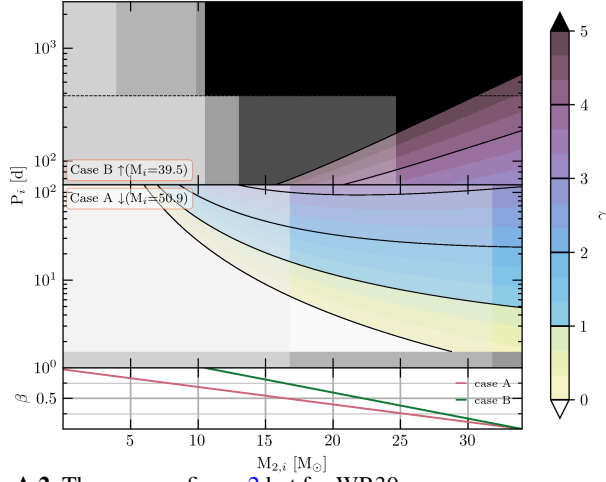
References

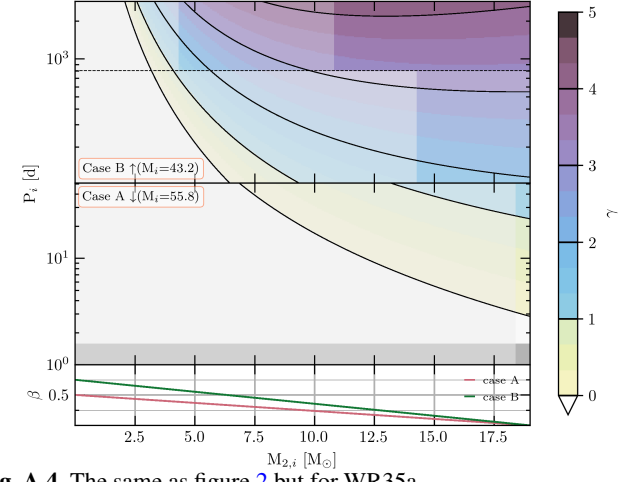
- Abbott, R., Abbott, T. D., Acernese, F., et al. 2023, *Physical Review X*, 13, 041039
- Almeida, L. A., Sana, H., Taylor, W., et al. 2017, *A&A*, 598, A84
- Banyard, G., Sana, H., Mahy, L., et al. 2022, *A&A*, 658, A69
- Barbá, R. H., Gamen, R., Arias, J. I., & Morrell, N. I. 2017, in *IAU Symposium*, Vol. 329, *The Lives and Death-Throes of Massive Stars*, ed. J. J. Eldridge, J. C. Bray, L. A. S. McClelland, & L. Xiao, 89–96
- Breivik, K., Coughlin, S., Zevin, M., et al. 2022, *COSMIC-PopSynth/COSMIC: COSMIC v3.4.7*
- Cherepashchuk, A. M. 2018, *Astronomy Reports*, 62, 567
- Collado, A., Gamen, R., & Barbá, R. H. 2013, *Astronomy & Astrophysics*, 552, A22
- Collado, A., Gamen, R., Barbá, R. H., & Morrell, N. 2015, *Astronomy & Astrophysics*, 581, A49
- Crowther, P. A. 2006
- de Mink, S. E., Pols, O. R., & Hilditch, R. W. 2007, *A&A*, 467, 1181
- Demers, H., Moffat, A. F. J., Marchenko, S. V., Gayley, K. G., & Morel, T. 2002, *The Astrophysical Journal*, 577, 409
- Dorozsmai, A. & Toonen, S. 2024, *MNRAS*, 530, 3706
- Dutta, D. & Klencki, J. 2024, *A&A*, 687, A215
- Eggleton, P. P. 1983, *The Astrophysical Journal*, 268, 368
- Evans, C. J., Taylor, W. D., Hénault-Brunet, V., et al. 2011, *A&A*, 530, A108
- Fahed, R., Moffat, A. F. J., Zorec, J., et al. 2011, *Monthly Notices of the Royal Astronomical Society*, 418, 2
- Gallegos-García, M., Fishbach, M., Kalogera, V., Berry, C. P. L., & Doctor, Z. 2022, *The Astrophysical Journal Letters*, 938, L19
- Gamen, R., Collado, A., Barbá, R., Chené, A. N., & St-Louis, N. 2014, *A&A*, 562, A13
- Ge, H., Webbink, R. F., Chen, X., & Han, Z. 2015, *The Astrophysical Journal*, 812, 40
- Klencki, J., Istrate, A., Nelemans, G., & Pols, O. 2022, *A&A*, 662, A56
- Klencki, J., Nelemans, G., Istrate, A. G., & Chruslinska, M. 2021, *Astronomy & Astrophysics*, 645, A54
- Klencki, J., Nelemans, G., Istrate, A. G., & Pols, O. 2020, *Astronomy & Astrophysics*, 638, A55
- Kobulnicky, H. A., Kiminki, D. C., Lundquist, M. J., et al. 2014, *ApJS*, 213, 34
- Lefèvre, L., Marchenko, S. V., Lépine, S., et al. 2005, *Monthly Notices of the Royal Astronomical Society*, 360, 141
- Lenoir-Craig, G., St-Louis, N., Moffat, A. F. J., & Pablo, H. 2021, *Monthly Notices of the Royal Astronomical Society*, 506, 4465
- Mahy, L., Rauw, G., De Becker, M., Eenens, P., & Flores, C. A. 2013, *A&A*, 550, A27
- Mandel, I. & Broekgaarden, F. S. 2022, *Living Reviews in Relativity*, 25, 1
- Martins, F. 2023, *A&A*, 680, A22
- Merle, T. 2024, *Bulletin de la Societe Royale des Sciences de Liege*, 93, 170
- Moe, M. & Di Stefano, R. 2017, *The Astrophysical Journal Supplement Series*, 230, 15
- Nelson, C. A. & Eggleton, P. P. 2001, *ApJ*, 552, 664
- North, J. R., Tuthill, P. G., Tango, W. J., & Davis, J. 2007, *Monthly Notices of the Royal Astronomical Society*, 377, 415

- Paczyński, B. 1967, *Acta Astron.*, 17, 355
- Paxton, B., Schwab, J., Bauer, E. B., et al. 2018, *The Astrophysical Journal Supplement Series*, 234, 34
- Petrovic, J., Langer, N., & van der Hucht, K. A. 2005, *Astronomy & Astrophysics*, 435, 1013
- Podsiadlowski, P., Joss, P. C., & Hsu, J. J. L. 1992, *ApJ*, 391, 246
- Pols, O. R. 1994, *A&A*, 290, 119
- Pols, O. R. & Marinus, M. 1994, *A&A*, 288, 475
- Richardson, N. D., Lee, L., Schaefer, G., et al. 2021, *The Astrophysical Journal*, 908, L3
- Sana, H., de Koter, A., de Mink, S. E., et al. 2013, *A&A*, 550, A107
- Sana, H., de Mink, S. E., de Koter, A., et al. 2012, *Science*, 337, 444
- Sen, K., Langer, N., Marchant, P., et al. 2022, *A&A*, 659, A98
- Shao, Y. & Li, X.-D. 2016, *The Astrophysical Journal*, 833, 108
- Shara, M. M., Crawford, S. M., Vanbeveren, D., et al. 2017, *MNRAS*, 464, 2066
- Soberman, G. E., Phinney, E. S., & Heuvel, E. P. J. v. d. 1997, *Stability Criteria for Mass Transfer in Binary Stellar Evolution*
- Tauris, T. M. & van den Heuvel, E. 2003, *Formation and Evolution of Compact Stellar X-ray Sources*
- Trigueros Páez, E., Barbá, R. H., Negueruela, I., et al. 2021, *A&A*, 655, A4
- van den Heuvel, E. P. J., Portegies Zwart, S. F., & de Mink, S. E. 2017, *Mon. Not. R. Astron. Soc.*, 471, 4256
- van der Hucht, K. A. 2001, *New Astronomy Reviews*, 45, 135
- van Rensbergen, W., De Greve, J. P., Mennekens, N., Jansen, K., & De Loore, C. 2010, *A&A*, 510, A13
- van Rensbergen, W., de Greve, J. P., Mennekens, N., Jansen, K., & de Loore, C. 2011, *A&A*, 528, A16
- Vanbeveren, D., De Donder, E., Van Bever, J., Van Rensbergen, W., & De Loore, C. 1998, *New A*, 3, 443
- Vanbeveren, D., Mennekens, N., Shara, M. M., & Moffat, A. F. J. 2018, *A&A*, 615, A65
- Vanbeveren, D., Mennekens, N., van den Heuvel, E. P. J., & Bever, J. V. 2020, *Astronomy & Astrophysics*, 636, A99
- Villaseñor, J. I., Taylor, W. D., Evans, C. J., et al. 2021, *MNRAS*, 507, 5348
- Wellstein, S. & Langer, N. 1999, *Implications of massive close binaries for black hole formation and supernovae*
- Wellstein, S., Langer, N., & Braun, H. 2001, *A&A*, 369, 939

Average ang. mom. loss γ for WR21, where $M_{WR}=19$, $M_O=37$, $P=8.25$

Fig. A.1. The same as figure 2 but for WR21.

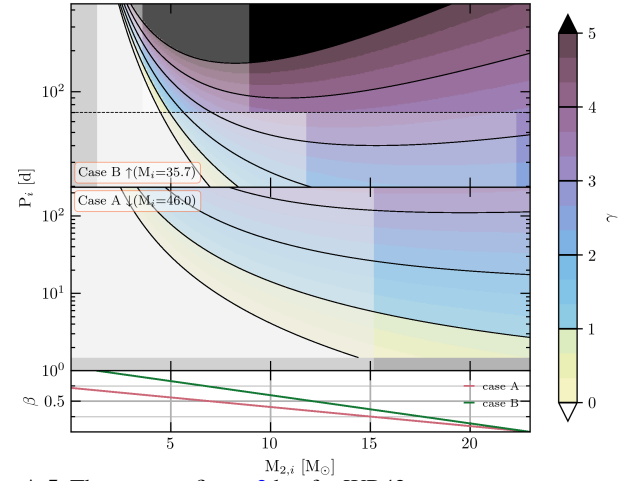
Average ang. mom. loss γ for WR31, where $M_{WR}=11$, $M_O=24$, $P=4.83$

Fig. A.3. The same as figure 2 but for WR31.

Average ang. mom. loss γ for WR30, where $M_{WR}=16$, $M_O=34$, $P=18.8$

Fig. A.2. The same as figure 2 but for WR30.

Average ang. mom. loss γ for WR35a, where $M_{WR}=18$, $M_O=19$, $P=41.9$

Fig. A.4. The same as figure 2 but for WR35a.

Appendix A: Additional system figures

In this section additional figures for the systems not discussed in section 4.1 can be found.

Average ang. mom. loss γ for WR42, where $M_{WR}=14$, $M_O=23$, $P=7.89$

Fig. A.5. The same as figure 2 but for WR42.

Average ang. mom. loss γ for WR48, where $M_{WR}=18$, $M_O=29$, $P=19.14$

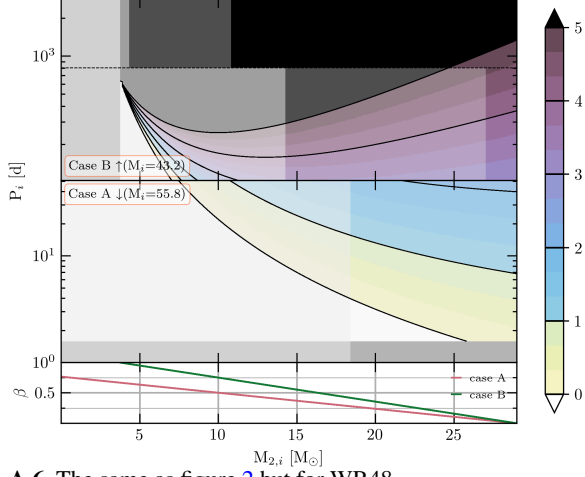


Fig. A.6. The same as figure 2 but for WR48.

Average ang. mom. loss γ for WR79, where $M_{WR}=11$, $M_O=29$, $P=8.89$

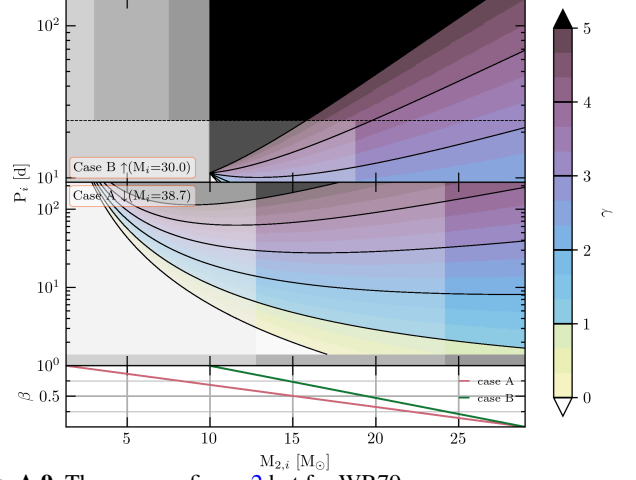


Fig. A.9. The same as figure 2 but for WR79.

Average ang. mom. loss γ for WR62a, where $M_{WR}=22.15$, $M_O=40.25$, $P=9.1$

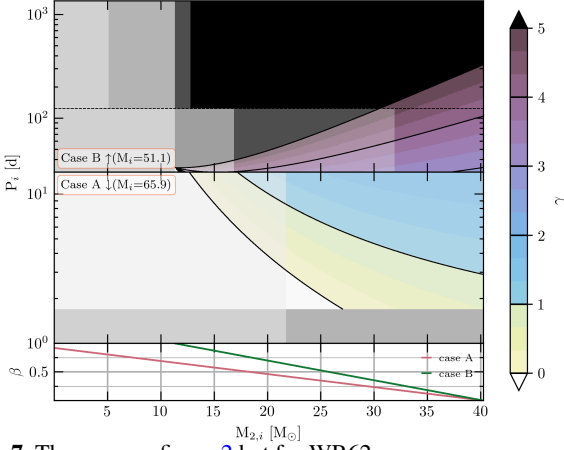


Fig. A.7. The same as figure 2 but for WR62a.

Average ang. mom. loss γ for WR127, where $M_{WR}=17$, $M_O=36$, $P=9.56$

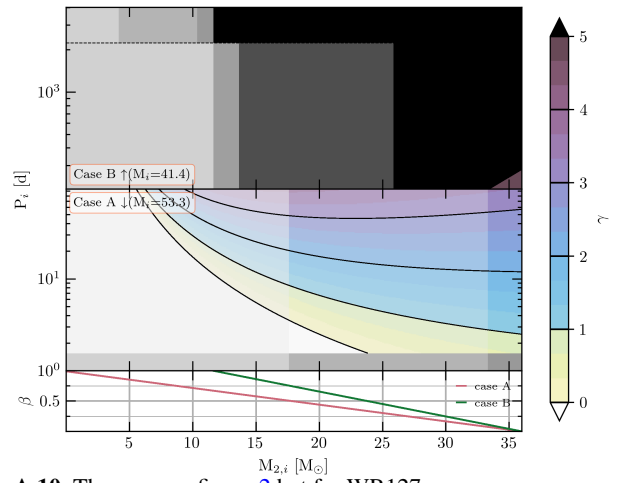


Fig. A.10. The same as figure 2 but for WR127.

Average ang. mom. loss γ for WR68a, where $M_{WR}=15$, $M_O=30$, $P=5.22$

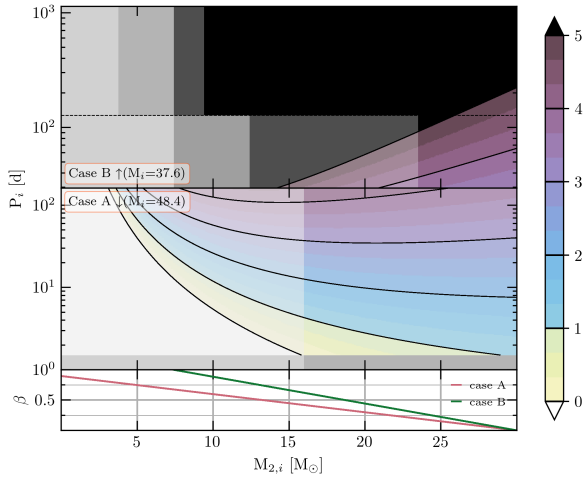


Fig. A.8. The same as figure 2 but for WR68a.

Average ang. mom. loss γ for WR139, where $M_{WR}=9.3$, $M_O=28$, $P=4$

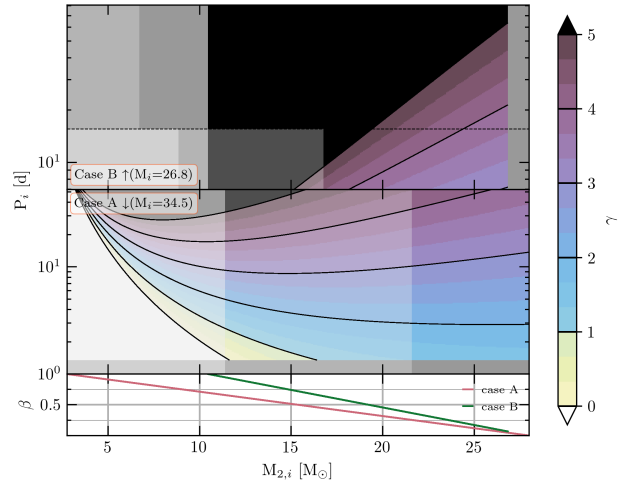
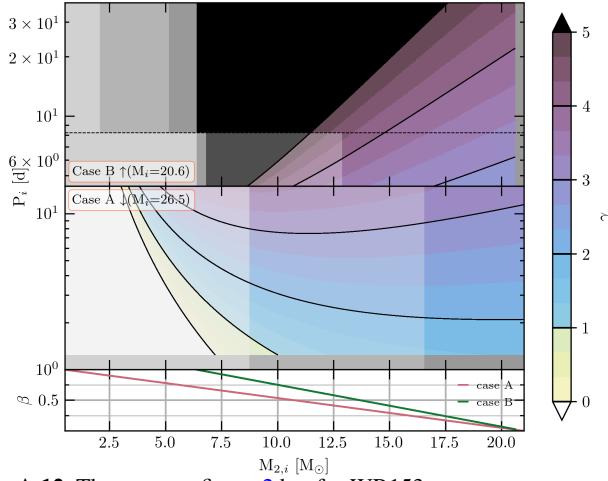
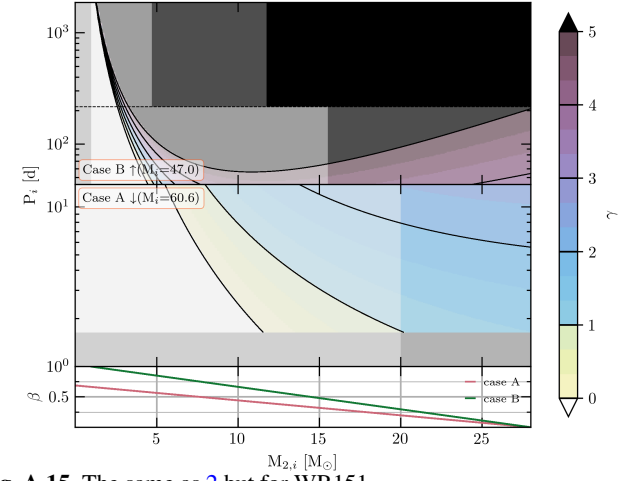
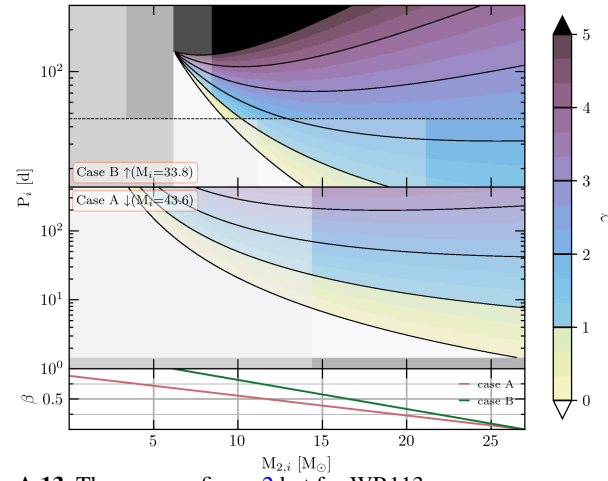
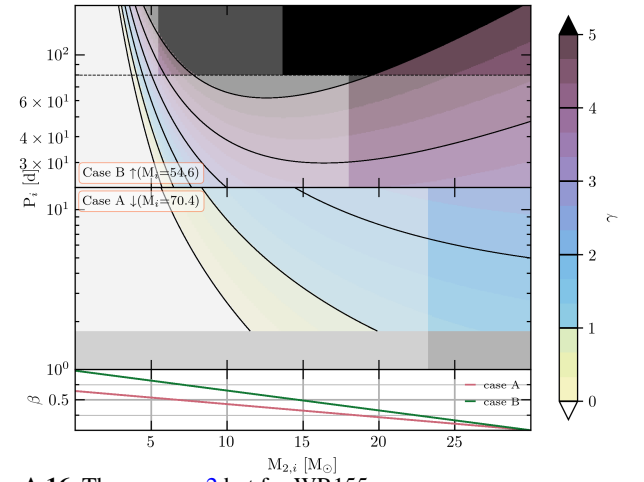


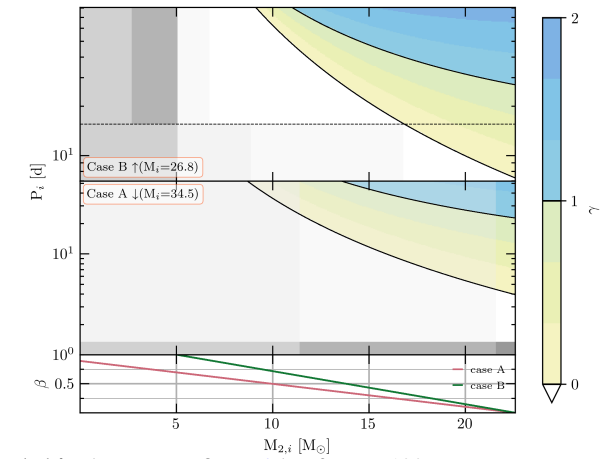
Fig. A.11. The same as figure 2 but for WR139.

Average ang. mom. loss γ for WR153, where $M_{WR}=6$, $M_O=21$, $P=3.47$

Fig. A.12. The same as figure 2 but for WR153.

Average ang. mom. loss γ for WR151, where $M_{WR}=20$, $M_O=28$, $P=2.13$

Fig. A.15. The same as 2 but for WR151.

Average ang. mom. loss γ for WR113, where $M_{WR}=13$, $M_O=27$, $P=29.7$

Fig. A.13. The same as figure 2 but for WR113.

Average ang. mom. loss γ for WR155, where $M_{WR}=24$, $M_O=30$, $P=1.64$

Fig. A.16. The same as 2 but for WR155.

Average ang. mom. loss γ for WR133, where $M_{WR}=9.3$, $M_O=22.6$, $P=112.8$

Fig. A.14. The same as figure 2 but for WR133.